© 2008 Nature Publishing Group http://www.nature.com/naturemethods

Colloid-guided assembly of oriented 3D neuronal networks

Sophie Pautot[1,2], Claire Wyart[1] & Ehud Y Isacoff[1]

A central challenge in neuroscience is to understand the formation and function of three-dimensional (3D) neuronal networks. *In vitro* studies have been mainly limited to measurements of small numbers of neurons connected in two dimensions. Here we demonstrate the use of colloids as moveable supports for neuronal growth, maturation, transfection and manipulation, where the colloids serve as guides for the assembly of controlled 3D, millimeter-sized neuronal networks. Process growth can be guided into layered connectivity with a density similar to what is found *in vivo*. The colloidal superstructures are optically transparent, enabling remote stimulation and recording of neuronal activity using layer-specific expression of light-activated channels and indicator dyes. The modular approach toward *in vitro* circuit construction provides a stepping stone for applications ranging from basic neuroscience to neuron-based screening of targeted drugs.

The central nervous system is a dense, layered, 3D interconnected network of neuronal cells, in which every neuron makes hundreds to thousands of specific connections with nearby and remote cognate partners[1]. This high connectivity permits the spiking dynamics and throughput that are essential for information processing[2–5]. However, most studies of neuronal connectivity *in vitro* have been limited to observations of small numbers of cells in dissociated two-dimensional (2D) cultures or in slice culture[6–16]. To understand the principles of circuit formation and dynamics in native neural tissue, *in vitro* methods have to be developed that allow control of cell density, connectivity and gene expression in three dimensions, as well as noninvasive recording and stimulation of individual neurons. Existing tissue engineering methods provide limited control and accessibility to the neuronal network[17–22], whereas methods involving transfected neurons co-cultured with brain slices allow the study of the formation of connections but rely on slice cultures[23].

Here we describe a method that makes it possible to grow dissociated cultured neurons on silica beads. The beads provide a growth surface large enough for neuronal cell bodies to adhere and for their processes to grow, mature and produce pre- and post-synaptic specializations. The use of these beads allowed us to move, transfect and culture highly differentiated neurons without disrupting their adhesion and without damaging their delicate processes. Moreover, we took advantage of the spontaneous assembly properties of monodispersed beads[24,25] to form 3D layered hexagonal arrays containing distinct subsets of neurons in different layers with constrained connectivity between neurons on different beads. We layered beads coated with a chemical attractant on a coverslip to promote axonal growth and orient functional neuronal connections between different bead layers. The use of optically transparent beads allowed us to interrogate network connectivity by optical imaging and to stimulate neurons containing fluorescent indicators and light-activated channels. Overall, the method allowed varied and complex layering of neurons, which can be differentially transfected and can connect functionally in the same layer or in different layers at distinct times.

RESULTS

Beads allow modular assembly of 3D networks

We used silica beads larger than 45 μm in diameter to provide a growth surface large enough for neuronal cell bodies and their processes. We coated the bead surface with poly(L-lysine) (PLL) to enhance cell adhesion and to support neuronal maturation[26,27]. We collected primary rat hippocampal neurons and cultured them on PLL-coated beads. The beads contained between one and a few neurons and glial cells. We dropped beads either onto coverslips containing conventional 2D neuronal cultures or onto bare coverslips upon which the monodispersed beads[24,25] assembled spontaneously into 2D ordered arrays (**Fig. 1a**).

To illustrate the assembly principle, after 2 days of *in vitro* culture, we used lentiviral infection to express GFP in one bead culture and tandem dimer Tomato (tdTomato) in another. Once the neurons reached maturity on their respective beads, we carefully moved the beads carrying the cells to small wells with a coarse pipette. The beads settled under gravitational force and spontaneously assembled into 2D hexagonal arrays at the bottom of the wells (**Fig. 1b**). Once the first layer was fully packed, we added more beads, which formed a second ordered layer that had the same

[1]Department of Molecular and Cell Biology, Life Science Addition 271, Mail Code 3200, University of California, Berkeley, and Physical Bioscience Division, Lawrence Berkeley National Laboratory, Berkeley, California 94720, USA. [2]Center for Regenerative Therapies Dresden, Tatzberg 47/49, 01307 Dresden, Germany. Correspondence should be addressed to E.Y.I. (ehud@berkeley.edu).

RECEIVED 16 FEBRUARY; ACCEPTED 27 JUNE; PUBLISHED ONLINE 20 JULY 2008; DOI:10.1038/NMETH.1236

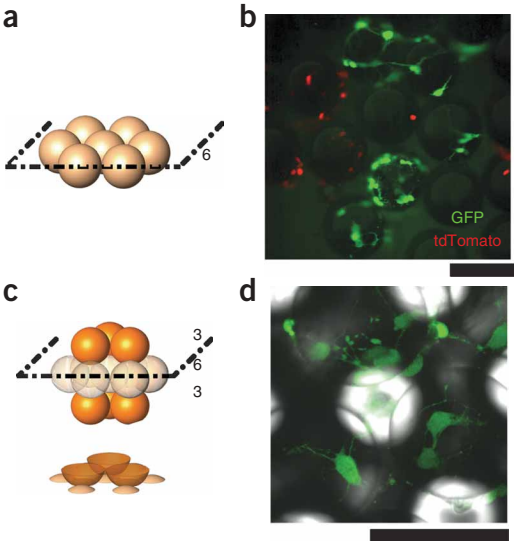

Figure 1 | Growth and manipulation of neurons growing on silica beads. (**a**) Schematic representation of spontaneous 2D bead assembly. (**b**) Two sets of neurons cultured on beads were infected on day 2 of *in vitro* culture with lentivirus driving the expression of GFP or of tdTomato. The two bead populations were mixed together on day 4 of *in vitro* culture and they spontaneously formed a 2D ordered array of green and red fluorescent neurons. (**c**–**d**) Two-layer assembly of beads carrying GFP-expressing neurons imaged live by confocal microscopy on day 4 of *in vitro* culture. Schematic representations (**c**) show the design of the bead assembly, with 3 layers (top) and a 20-μm-deep subsection of the assembly (bottom) that corresponds to the confocal image in **d**. The image is an *x*-*y* projection of a 20 μm (10 frames) confocal *z*-series images overlaid with the corresponding bright-field image. Scale bars, 125 μm.

hexagonal symmetry (**Fig. 1c**). Successive addition of beads resulted in construction of a packed 3D assembly (**Fig. 1d**).

After the spontaneous assembly of the 3D hexagonal arrays, neuronal processes grew between the beads over the course of 3 weeks in culture to form highly interconnected millimeter-sized networks without the use of conditioned medium or a glial feeder layer (**Fig. 2a**). To characterize the assemblies, we acquired confocal microscopy images of the arrays (**Fig. 2b** and **Supplementary Video 1** online). We observed neuronal processes crossing from one bead to the next and observed glial cells in all the bead layers (**Fig. 2a**). Despite the small number of glia on each bead, they were sufficient to maintain neuron health and support uniform and robust neuronal process outgrowth throughout the bead layers, including in the deep layers (**Fig. 2b**,**c**). The beads were woven together by the crossing processes and formed stable structures (**Fig. 2b**), eliminating the need for exogenous cross-linking agents to hold the arrays together during solution exchange. The void spaces between the beads permitted the necessary medium exchange to maintain healthy growing conditions. The number of cells per bead and the number of neuronal processes were similar in all layers of the array (**Fig. 2a**), indicating that cell health is not affected by location within the assembly.

Tuning bead size

By varying both the density of cells during plating and the dimension of the beads, we determined the density of cells per bead and thus the number of cells per unit volume in the arrays. Using the geometry of the assembly depicted in **Figure 1c**, we estimated the number of cells per unit volume in relation to both bead size and number of cells per bead (**Fig. 2c**). For a given volume, a hexagonal compact assembly of 45 μm diameter beads is composed of 19 times more beads than an assembly of 125 μm diameter beads. Under our seeding conditions a surface density of 75,000 cells/cm^2 corresponded to an average of 5 neurons per 45 μm diameter bead and about 35 neurons per 125 μm diameter bead. Therefore the cell density per cubic millimeter in the final assembly was about 2.7 times higher for the 45 μm diameter beads

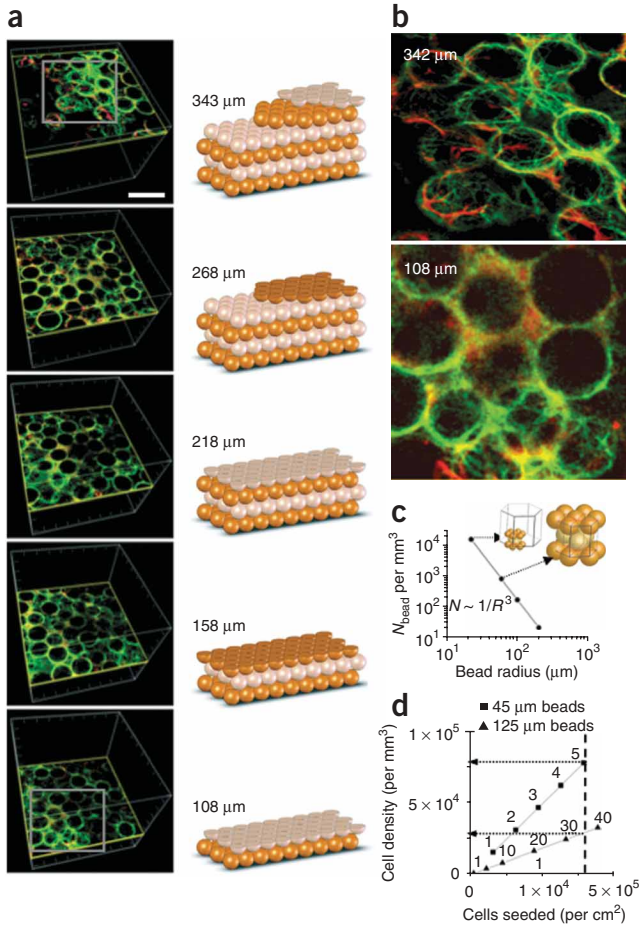

Figure 2 | Three-dimensional self-assembly of a neuronal network. (**a**) Three-week-old culture of 3D neuronal network assembly fixed and stained with the neuron-specific antibody to alpha tubulin (green) and the glial-specific antibody to GFAP (red). Five layers, a 450 × 450 × 388 μm volume of the assembly, were imaged by confocal microscopy. The images extracted from the *z* stack for the green and red channels (left) are shown with schematic representations of the corresponding layer position (right). Number refers to the position of the section within the *z* stack. Scale bar, 100 μm. (**b**) Expanded views of regions (rectangles) from top and bottom layers in **a** show the details of the cells and their processes wrapped around the beads. (**c**) Scaling of the number of beads per unit volume with bead size. The graph provides the number of beads per unit volume for beads with a radius of 22.5, 62.5, 100 and 200 μm. The schematic shows the volume filled by one hexagonal compact crystal motif (12 beads) with a 62.5-μm bead radius and the volume filled with the corresponding crystal motif (12 beads) for 22.5-μm-radius beads. (**d**) Relation between the volume density of cells and cell seeding conditions. Dashed lines are visual guides to point to the corresponding values on the axis. Each point is labeled with the corresponding number of cells per bead.

© 2008 Nature Publishing Group http://www.nature.com/naturemethods

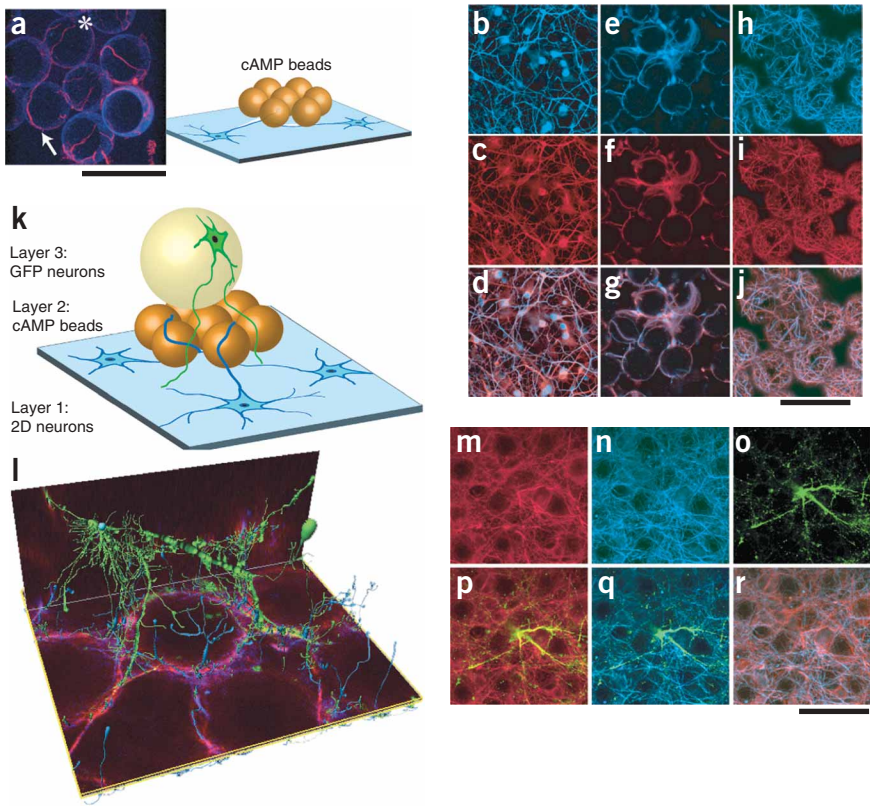

Figure 3 | Guidance of interlayer connections. (**a**) Neurons were cultured in two dimensions on a coverslip (layer 1) for ~1 week (5–7 d *in vitro*) before cAMP-coated 45 μm beads, which contained no neurons of their own, were layered on top of them (schematic on right). Three days later the culture was fixed and stained with smi-312, an axon-specific antibody (red). Confocal microscopy *z*-series images starting 5 μm above the 2D culture and ending at the top of the bead was projected in three dimensions (left). Axons from neurons on the coverslip grew onto the surface of the overlying cAMP-coated beads (arrow marks point where an axon leaves the coverslip for the bead surface; asterisk marks the end of the growing axon). (**b**–**j**) Axons from neurons on the coverslip (layer 1, **b**–**d**) represent most of the processes in the cAMP-coated beads (layer 2) 2 d after the bead layer is formed (**e**–**g**), and these grow extensively over the next 5 d (**h**–**j**). Cells were fixed and stained for neuronal (Tuj-1, red) and axonal (smi-312, blue) markers 2 d (**b**–**g**) or 7 d (**h**–**i**) after addition of the cAMP bead layer. (**k**–**r**) GFP-expressing neurons in a layer of beads (layer 3 was added 2 d after layer 2) extend dendrites down through the cAMP bead layer. Schematic of arrangement of three layers (**k**). A 3D reconstruction of axons (blue) from neurons on the coverslip (layer 1) growing up into the intermediate layer of cAMP beads (layer 2) and encountering there descending dendrites from bead layer (layer 3) of GFP-expressing cells (green) (**l**). (**m**–**r**) The dendrites of the GFP cells in layer 3 reached down as far as layer 1. Optical sections shown only in layer 1, labeled for all processes (Tuj-1, red; **m**,**p**), axons (smi-312, blue; **n**,**q**) and GFP from upper layer 3 (green; **o**–**r**). In **m**–**o** individual fluorescence channel is shown and **p**–**r** show merged channels. Scale bars, 100 μm.

© 2008 Nature Publishing Group http://www.nature.com/naturemethods

(**Fig. 2d**). Hence, the most effective way to increase cell density, while allowing for a low number of cells per bead, is to use small beads (**Fig. 2d**). The upper limit to cell density is dictated by the free volume left by beads and is defined by bead packing order, representing 32% of the total volume for hexagonal compact assembly. We achieved densities of up to 75,000 cells/mm^3 with 45 μm diameter beads, that is, close to the 91,000 cells/mm^3 measured in the mouse brain cortex[28].

The pattern of connectivity between neurons on beads within a 3D hexagonal array was spatially constrained by the 12 equidistant contacts made between each bead and its neighbors: 6 within the plane, 3 in the plane above and 3 in the plane below (**Fig. 2a**). For hexagonal ordered assemblies, the density of connection points depends inversely on the bead radius cubed, and the distance between contact points is linearly related to the bead radius. Thus, the neuronal connectivity of the network that forms on these bead arrays is expected to be set by bead size, with smaller beads leading to assemblies with higher connectivity.

Directed growth guides interlayer axodendritic connectivity

We aimed to guide process extension from one population of neurons to another by inserting guiding beads in the assembly. We first coated beads with the attractant signaling molecule cyclic AMP (cAMP), which guides axonal growth[29]. We assembled the coated beads not carrying cells into a single-layer packed array on top of a coverslip supporting a neuronal culture (**Fig. 3a**). Axons from neurons that encountered a cAMP-coated bead adhered to the bead and grew upward at a rate of ~50 μm/d, extending over the bead surface. This rate of growth showed no obvious dependence on bead size. Because the distance between bead contacts is proportional to bead radius, axons bridged to neighboring beads more quickly on the smaller 45 μm beads. Within 3 d the axons grew over the surface of the 45 μm beads and reached the contact points with as many as three neighboring beads, with each such contact affording an opportunity to extend to the neighboring bead (**Fig. 3a**).

The axon-guidance effect of cAMP was strongest in the first 2 d after deposition of the cAMP-coated bead layer. Staining for the neurite marker, Tuj-1 (which stains both axons plus dendrites) and for the axon-specific marker, smi-312, verified that axons grew upward from the neurons and onto the beads. Axons were readily distinguished on the coverslip (layer 1) among all of the neurites (**Fig. 3b–d**). In the first 2 d after adding the cAMP-coated beads, the only processes that grew onto the beads from the neurons on the coverslip were axons (**Fig. 3a**,**e**–**g**). However, after 7 d in culture, dendrites from the neurons on the coverslip (layer 1) also appeared on the cAMP-coated beads of layer 2 (**Fig. 3h–j** and **Supplementary Video 2** online), indicating a loss of axonal specificity over time. Five days after depositing the cAMP beads, we added a second bead layer (layer 3), which contained neurons expressing GFP (**Fig. 3k** and **Supplementary Fig. 1** online). As by this time the cAMP-coated beads were no longer selectively attractive to axons,

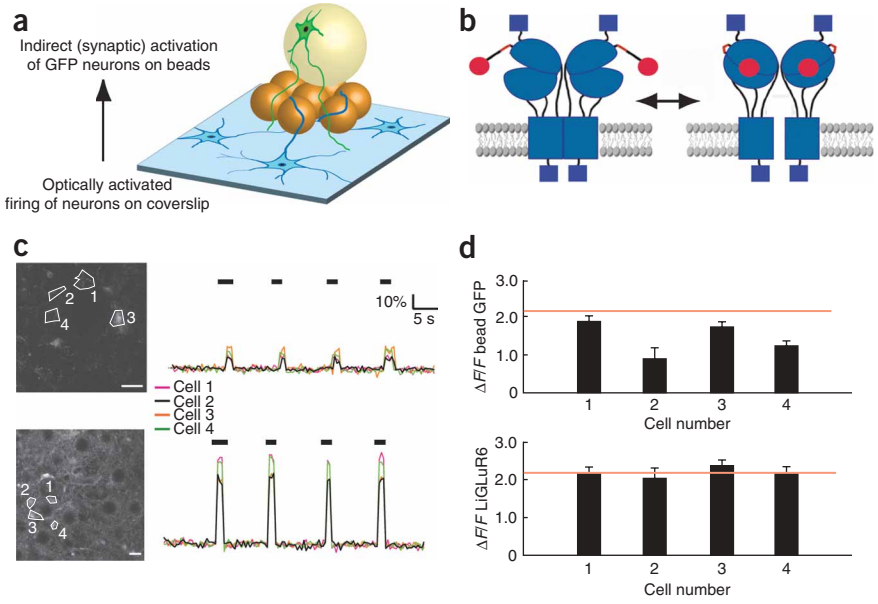

Figure 4 | Functional synaptic connectivity between neuronal layers. (**a**) Schematic of the directed 3D neuronal assembly. Neurons cultured on a coverslip (blue) were transfected with LiGluR6. One week later the layer of cAMP-coated beads was added as a guidance layer (layer 2, orange). After 2 d of growth of axons from the coverslip into the layer 2 beads, a third layer of beads carrying neurons infected with GFP was added. These GFP-expressing neurons extended dendrites down into layer 2 and met the axons of layer 1. (**b**) A schematic of LiGluR6 in the cell membrane of the coverslip neurons in both resting state, where the MAG photoswitch is in the *trans* state and points its glutamate away from the binding pocket, and after illumination with violet light (390 nm), which photoswitches the MAG into the *cis* state, allowing the glutamate to bind and open the channel, leading to influx of Ca^{2+} to excite the neuron. (**c**,**d**) Photoswitching of neuronal activity as detected by rises in Ca^{2+} was measured using the rhod-2 indicator. Illumination with 390-nm light excited the LiGluR6-expressing neurons on the coverslip (bottom image and rhod-2 fluorescence traces), and illumination at 543 nm turned the excitation off. Traces correspond to rhod-2 fluorescence change ($\Delta F/F$) as illumination changes. Bars above traces indicate timing of illumination at 390 nm. Optical stimulation also excites GFP-expressing layer-3 neurons (top image and traces), which do not express LiGluR, indicating that they receive excitatory inputs from layer 1. Responses for four cells on coverslip and four cells on a bead in layer 3 are color coded, as indicated, and superimposed. Lines in **d** indicate the mean $\Delta F/F$ for LiGluR6 neurons. Bead GFP refers to cells from layer 3. Error bars, s.e.m.; $n = 10$. Scale bars, 35 μm.

GFP-positive dendrites from layer 3 extended onto intermediate layer 2 where they encountered the axons from layer 1. This could be seen from the reconstruction of confocal *z*-series images using filament tracing software (**Fig. 3l**). Processes from GFP-expressing cells in layer 3 that reached layer 1 were only stained by Tuj-1 (**Fig. 3m–r**), indicating that only the dendrites of layer 3 cells reached the bottom layer. Staining with smi-312s showed that axons from the bottom layer climbed up into the guidance layer (layer 2) to reach the upper-layer (layer 3) GFP neurons (**Fig. 3l**). Thus, an intermediate layer of cAMP-coated beads can be used to mediate directional connections between neurons growing in layers above and below during the course of the first week of contact. We observed a similar connectivity pattern on other beads (**Supplementary Fig. 2** online). Although this pattern of connectivity was set up at 7 d, in long-term culture it would likely evolve depending on the influence of activity and other molecular cues.

Functional synaptic connections between neuron layers

We next asked whether the contacts between axons from layer 1 and dendrites from layer 3 constituted functional synapses. To test this we used the light-gated glutamate receptor (LiGluR6), containing an attachment site for the photoswitched tethered glutamate molecule MAG-1 (refs. 30–32). We transfected LiGluR6 into the neurons on the coverslip several days before adding the guiding bead layer. On top of the cAMP-coated beads we then layered beads that carried neurons expressing GFP. At 12 d *in vitro* we labeled neurons with the tethered photoswitch MAG-1 and the calcium-sensitive fluorescent indicator rhod-2. MAG-1 selectively confers optical excitation only onto neurons expressing LiGluR6 (ref. 32). The rhod-2 dye loaded into both layers of neurons, enabling us to use confocal Ca^{2+} imaging to monitor neuronal activity. We designed this cell layout (**Fig. 4a**) to selectively stimulate the coverslip neurons with light, while monitoring activity in both layers: layer 1 with LiGluR6 neurons and upper layer 3 with neurons that did not express LiGluR6 but expressed GFP.

We activated LiGluR6 by illumination at 390 nm (using a frequency-doubled 780-nm pulsed laser) and turned the activity off by illumination at 543 nm (**Fig. 4b**). Illumination with the shorter-wavelength light reliably and repeatedly triggered an influx of Ca^{2+} into the LiGluR6-expressing neurons on the coverslip, whereas illumination with the longer visible-wavelength light turned this activity off and resulted in a return to resting Ca^{2+} concentrations (**Fig. 4c**). Neurons that do not express LiGluR6 but are labeled with MAG-1 are not activated by illumination at 390 nm[32]. Ca^{2+} imaging of the GFP layer of neurons on the beads revealed that they too were activated by illumination at 390 nm and deactivated at 543 nm (**Fig. 4c**), even though they did not express LiGluR6, indicating the existence of functional synapses between the two layers, with the neurons on the coverslip being presynaptic.

The all-optical approach to stimulating and recording activity enabled us to ask whether the circuit properties are uniform or heterogeneous across an *in vitro* 3D neuronal array. We found that although neurons on the coverslip responded reliably and similarly to optical stimulation, the GFP-expressing cells on the beads sometimes responded similarly (**Fig. 4c**) and at other times showed responses that differed in strength from neuron to neuron, even on the same bead (**Fig. 4d**). This demonstrated that it is possible to use the all-optical approach of light-gated ion channels and activity indicators to assess the spatial and temporal properties of synaptic transmission in the 3D neuronal arrays. This method provides a dynamic range of detection that can reveal heterogeneities in synaptic strength and therefore, in principle, should make it possible to study how functional connectivity is regulated by the history of chemical, molecular or electrical activity.

© 2008 Nature Publishing Group http://www.nature.com/naturemethods

© 2008 Nature Publishing Group http://www.nature.com/naturemethods

DISCUSSION

In recent years, scientists have used tissue engineering in attempts to create 3D neuronal cultures that emulate the high cell density and connectivity seen *in vivo* by using two main approaches to biomaterials: polymer gels and solid porous matrices[17–22]. Polymer gels molded to form tubes have been used successfully to provide 2D growth surfaces for peripheral neurons and to protect their processes from the inflammatory response of surrounding scar tissue[18,19]. When cast as uniform blocks with cells embedded in them, they have provided supports for 3D cultures of neurospheres (neuronal stem cell aggregates)[22]. Polymer gels have not been applied to isolated primary neurons. Moreover, to create layered 3D cultures from polymer gels would require gel microprinting, and it would be difficult to place cells of different types in desired 3D relations to one another. Although the use of solid porous matrices is attractive because of their rigid mechanical properties[20,21], these matrices have limited porosity, and thus they do not allow for deep cell migration within the matrix. This could be overcome by grinding or slicing the matrix into 'unit' modules, but the diversity of size and shape of the particles would be expected to interfere with packing into regular layered arrays.

In contrast to other methods, our approach makes it possible to grow dissociated neurons on moveable surfaces that allow for genetic and mechanical manipulation and assembly into ordered 3D networks. We worked with silica beads that are large enough to provide an adhesion surface for neuronal cell bodies, and for growth and differentiation of axons and dendrites. The neurons can be moved by displacing the beads without disrupting cell adhesion or damaging the delicate processes. They can be transfected before transfer either into culture dishes containing conventional 2D neuronal cultures, with which they form contacts, or in such a way that they spontaneously organize into regular ordered 2D layers. Layers can be added in succession to make 3D hexagonal arrays. Some of the layers can contain beads coated with chemical guidance cues that direct process growth to create synaptic layers. Finally, the ability to combine groups of cells that are differentially transfected makes it possible to express light-gated channels exclusively in one layer of neurons and use functional imaging to determine the development of functional connections between the light-activated layer and other neuronal layers. These properties of the colloid method make it possible to do what the earlier methods could not, namely, to build artificial layered networks out of genetically modified cells, under conditions that provide for cell densities that approach those found in the brain, and allowing synaptic connections to be formed and their spatial distribution and strength to be assessed.

Our method should pave the way for studying synapse formation and modification in the context of specific molecular interactions, chemical cues and activity patterns in designed 3D networks. Because the approach is amenable to long-term culture, it affords a unique system for cell-based assays of neurally targeted drugs and could prove useful for developmental studies of interactions between neurons in a controlled environment.

METHODS

Expression constructs. We replaced the *CMV* promoter of HIV-CS-CG-SynapsinPr-GFP by a synapsin promoter. We added a multi-cloning site (*Pst*I, *Xba*I *Pac*I and *Not*I) between the synapsin promoter and *GFP*. To obtain tdTomato-expressing lentivirus construction, we removed the gene encoding GFP using the *Xba*I restriction site and replaced it by a gene encoding tdTomato using the *Spe*I restriction site we added to the multicloning site present in the pRSETB_tdTomato plasmid.

Neuron culture on silica bead preparation. We sterilized borosilicate glass spheres (MO-SCI Specialty Products) in an ethanol solution overnight, and dried them under vacuum. Then we incubated the beads in a borate buffer solution for 1 h and placed them in PLL solution overnight. We removed hippocampi from embryonic day 18 (E18) rats, treated them with trypsin for 20 min at 37 °C, and then washed and triturated them. For the direct 3D assembly of macroscopic networks, we plated dissociated cells at 75,000 cells/cm^2 on poly(lysine)-coated glass beads and cultured them in neurobasal medium supplemented with 2 mM Glutamax, 2% fetal bovine serum (FBS) and 2% B-27 for the first week, and suppressed FBS for the following weeks to keep glia cell division to a minimum. As a result, the networks had scattered endogenous glial cells (**Fig. 2b–c**), which provide local sources of conditioning and support healthy growth for weeks. For guided assembly, we plated at 50,000 cells/cm^2 to keep cell density on each bead to a minimum, kept neurons in FBS-free medium, and supplemented the medium with conditioned medium from 1-week-old hippocampal cultures.

We seeded cells as typical for 2D cultures. We counted dissociated cells in a given volume in a hemacytometer and from this value calculated the total number of cells for the entire volume. We added this volume with a known number of cells to PLL-coated beads close packed in a single layer on a polycarbonate membrane (tissue culture insert). Most of the *x-y* surface upon which the cells could drop ($\sim$85%) was occupied by the beads so that the majority of cells ended up on the beads. We calculated the cell density on the beads based on the total surface area of each bead multiplied by the number of beads.

We transfected the cells using Lipofectamine 2000 (Invitrogen) or by infecting them with lentivirus after 2–15 d after dissociation and analyzed them 2–14 d after infection.

To build the intermediate guidance layer, we physisorbed fluorescently labeled cAMP onto PLL-coated beads. The cAMP was still visible on the beads after 7 d in culture, indicating that it remained adsorbed, even though the selective attraction of axons was lost.

Immunostaining. We purchased antibodies to alpha-tubulin and to GFAP from Chemicon International. We obtained anti–smi-312 and anti–Tuj-1 from Covance.

MAG labeling and illumination protocol. We conjugated MAG-1 to iGluR6(L439C) in hippocampal neurons for optical switching experiments in a procedure based on a previously described method[32]. We diluted the compound to 25 μM in a solution containing 150 mM *N*-methyl-D-glucamine-HCl (NMDG-HCl), 3 mM KCl, 0.5 mM $CaCl_2$, 5 mM $MgCl_2$, 10 mM HEPES, 5 mM glucose (pH 7.4), and preactivated it by UV light (365 nm) for 1 min to enhance conjugation by affinity labeling[31]. We incubated a coverslip containing beads in the dark in 200 μl of the labeling solution for 15 min at 37 °C. Then we loaded the cells for 10–15 min with rhod-2 (Molecular Probes) at 5 μM in 20% pluronic acid and washed the slides three times with the extracellular recording solution. After a 15-min recovery

period, we examined the cultures to confirm that the neuronal networks on beads were intact.

We imaged the preparation on an inverted confocal microscope (Zeiss LSM 510 Axiovert 200) using a 40×, 1.3 numerical aperture (NA) oil objective. We illuminated the neurons with 390-nm light (frequency doubled 780 nm) to activate LiGluR6, and with 543 nm illumination both to image rhod-2 and to deactivate LiGluR6.

Imaging. We acquired confocal microscopy *z*-series images on a Zeiss LSM510 confocal microscope with 63× dipping objective (0.9 NA), and a Zeiss 5-Live confocal microscope with 20× dipping objective. We selected laser power, photomultiplier gain and filter sets to minimize bleaching and bleed-through between channels (Alexa488 and GFP: excitation, 488 nm and emission, 500–550 nm; Cy3: excitation, 543 nm and emission, 565–615 nm; Alexa 647: excitation, 633 nm and emission, 650–700 nm).

Note: Supplementary information is available on the Nature Methods website.

ACKNOWLEDGMENTS

We thank E. Callaway (Salk Institute) for the lentiviral DNA constructs (HIV-CS-CG-SynapsinPr-GFP), R. Tsien (University of California, San Diego) for the pRSETB_tdTomato plasmid, K. Kolstad and J. Flannery (University of California, Berkeley) for providing us with the AAV-SynapsinPr-LiGluR virus and for assisting in the preparation of the lentivirus, the Molecular Imaging Center and H. Aaron for help with the confocal microscopy, and M.M. Poo, M. Shelly, M.B. Forstner and S. Kohout for helpful discussions and comments. This work was supported by the US National Institutes of Health Nanomedicine Development Center in Optical Control of Biological Function (PN2 EY1018241). C.W. was supported by a Marie Curie Outgoing International Fellowship funded through Laboratoire de Neurosciences et Systèmes Sensoriels, Centre National de la Recherche Scientifique, Uniteé Mixte de Recherche 5020.

AUTHOR CONTRIBUTIONS

S.P. designed and executed experiments; C.W. contributed to the light-gated ion channel experiments; and E.Y.I. supervised the project.

Published online at http://www.nature.com/naturemethods/
Reprints and permissions information is available online at http://npg.nature.com/reprintsandpermissions/

© 2008 Nature Publishing Group http://www.nature.com/naturemethods

1. Beaulieu, C. & Colonnier, M. The number of neurons in the different laminae of the binocular and monocular regions of area 17 in the cat, Canada. *J. Comp. Neurol.* **217**, 337–344 (1983).
2. Shepherd, G.M. Microcircuits in the nervous system. *Sci. Am.* **238**, 93–103 (1978).
3. Shepherd, G.M. The synaptic organization of the brain. (Oxford University Press, New York, 1979).
4. Changeux, J.P. & Dehaene, S. Neuronal models of cognitive functions. *Cognition* **33**, 63–109 (1989).
5. Golomb, D. & Hansel, D. The number of synaptic inputs and the synchrony of large, sparse neuronal networks. *Neural Comput.* **12**, 1095–1139 (2000).
6. Ikeda, S.R. Expression of G-protein signaling components in adult mammalian neurons by microinjection. *Methods Mol. Biol.* **259**, 167–181 (2004).
7. Miyoshi, H., Blomer, U., Takahashi, M., Gage, F.H. & Verma, I.M. Development of a self-inactivating lentivirus vector. *J. Virol.* **72**, 8150–8157 (1998).
8. Wickersham, I.R., Finke, S., Conzelmann, K.K. & Callaway, E.M. Retrograde neuronal tracing with a deletion-mutant rabies virus. *Nat. Methods* **4**, 47–49 (2007).
9. Wickersham, I.R. *et al.* Monosynaptic restriction of transsynaptic tracing from single, genetically targeted neurons. *Neuron* **53**, 639–647 (2007).
10. Lo, Y.J. & Poo, M.M. Heterosynaptic suppression of developing neuromuscular synapses in culture. *J. Neurosci.* **14**, 4684–4693 (1994).
11. Wyart, C. *et al.* Constrained synaptic connectivity in functional mammalian neuronal networks grown on patterned surfaces. *J. Neurosci. Methods* **117**, 123–131 (2002).
12. Chiappalone, M. *et al.* Networks of neurons coupled to microelectrode arrays: a neuronal sensory system for pharmacological applications. *Biosens. Bioelectron.* **18**, 627–634 (2003).
13. Hofmann, F. & Bading, H. Long term recordings with microelectrode arrays: studies of transcription-dependent neuronal plasticity and axonal regeneration. *J. Physiol. (Paris)* **99**, 125–132 (2006).
14. Morin, F. *et al.* Constraining the connectivity of neuronal networks cultured on microelectrode arrays with microfluidic techniques: a step towards neuron-based functional chips. *Biosens. Bioelectron.* **21**, 1093–1100 (2006).
15. Xiang, G. *et al.* Microelectrode array-based system for neuropharmacological applications with cortical neurons cultured *in vitro*. *Biosens. Bioelectron.* **22**, 2478–2484 (2007).
16. Jun, S.B. *et al.* Low-density neuronal networks cultured using patterned poly-l-lysine on microelectrode arrays. *J. Neurosci. Methods* **160**, 317–326 (2007).
17. Lee, J., Cuddihy, M.J. & Kotov, N.A. Three-dimensional cell culture matrices: state of the art. *Tissue Eng. Part B: Reviews* **14**, 61–86 (2008).
18. Schmidt, C.E. & Leach, J.B. Neural tissue engineering: strategies for repair and regeneration. *Annu. Rev. Biomed. Eng.* **5**, 293–347 (2003).
19. Huang, Y.C. & Huang, Y.Y. Biomaterials and strategies for nerve regeneration. *Artif. Organs* **30**, 514–522 (2006).
20. Shany, B., Vago, R. & Baranes, D. Growth of primary hippocampal neuronal tissue on an aragonite crystalline biomatrix. *Tissue Eng.* **11**, 585–596 (2005).
21. Baranes, D. *et al.* Interconnected network of ganglion-like neural cell spheres formed on hydrozoan skeleton. *Tissue Eng.* **13**, 473 (2007).
22. Ma, W. *et al.* CNS stem and progenitor cell differentiation into functional neuronal circuits in three-dimensional collagen gels. *Exp. Neurol.* **190**, 276–288 (2004).
23. Polleux, F. & Ghosh, A. The slice overlay assay: a versatile tool to study the influence of extracellular signals on neuronal development. *Sci. STKE* **136**, l9 (2002).
24. Pusey, P.N. & Vanmegen, W. Phase-behavior of concentrated suspensions of nearly hard colloidal spheres. *Nature* **320**, 340–342 (1986).
25. van Blaaderen, A., Ruel, R. & Wiltzius, P. Template-directed colloidal crystallization. *Nature* **385**, 321–324 (1997).
26. Letourneau, P.C. Cell-to-substratum adhesion and guidance of axonal elongation. *Dev. Biol.* **44**, 92–101 (1975).
27. Letourneau, P.C. Possible roles for cell-to-substratum adhesion in neuronal morphogenesis. *Dev. Biol.* **44**, 77–91 (1975).
28. Abeles, M. *Corticonics: Neural Circuits of the Cerebral Cortex*. (Cambridge University Press, New York, 1991).
29. Song, H.J., Ming, G.L. & Poo, M.M. cAMP-induced switching in turning direction of nerve growth cones. *Nature* **388**, 275–279 (1997).
30. Volgraf, M. *et al.* Allosteric control of an ionotropic glutamate receptor with an optical switch. *Nat. Chem. Biol.* **2**, 47–52 (2006).
31. Gorostiza, P. *et al.* Mechanisms of photoswitch conjugation and light activation of an ionotropic glutamate receptor. *Proc. Natl. Acad. Sci. USA* **104**, 10865–10870 (2007).
32. Szobota, S. *et al.* Remote control of neuronal activity with a light-gated glutamate receptor. *Neuron* **54**, 535–545 (2007).